PCCP

High-resolution VUV photoionization spectroscopy of HD between the X $^2\Sigma_g^+$ $v^+ = 0$ and $v^+ = 1$ thresholds†

G. M. Greetham,[a] U. Hollenstein,[a] R. Seiler,[a] W. Ubachs[b] and F. Merkt*[a]

[a] *Laboratorium für Physikalische Chemie, ETH Zürich, CH-8093, Zurich, Switzerland*
[b] *Laser Centre, Department of Physics and Astronomy, Vrije Universiteit, De Boelelaan 1081, 1081 HV, Amsterdam, The Netherlands*

Received 12th March 2003, Accepted 23rd April 2003
First published as an Advance Article on the web 9th May 2003

The photoionization spectrum of HD has been recorded in the region of the first vibrationally excited level ($v^+ = 1$) of the X $^2\Sigma_g^+$ ground state of the HD^+ ion using a narrow bandwidth vacuum ultraviolet (VUV) laser. Spectral positions, intensities and line widths are reported for all resonances observed between 126 100 and 126 700 cm^{-1}. The *n*p Rydberg series converging to the $v^+ = 1$, $N^+ = 0$ and 2 states of the ion have been observed up to $n = 150$ and used to determine the corresponding ionization thresholds in a multichannel quantum defect theory analysis. After subtraction of the ionic vibrational energy the adiabatic ionization energy of HD was determined to be 124 568.491 ± 0.017 cm^{-1}. Several low *n* interloper Rydberg states converging to higher vibrational levels ($v^+ > 1$) of HD^+ have also been observed and their interaction with the $v^+ = 1$ channel is discussed.

1 Introduction

The hydrogen molecule represents a test system for theories describing molecular structure, in particular *ab initio* quantum theory and multichannel quantum defect theory (MQDT). Whereas non-Born–Oppenheimer effects and mass-dependent adiabatic effects can be studied from the comparison of H_2 and D_2, the HD molecule gives access to the terms in the Hamiltonian imposing breakdown of inversion symmetry.[1]

Experimental values for the adiabatic ionization energy (IE) and the dissociation energy[2] of HD represent key quantities to test theoretical predictions. The most accurate experimental IE for HD is that reported by Gilligan, Eyler and co-workers, who extrapolated the *n*p Rydberg series converging to the ground rovibronic X $^2\Sigma_g^+$ ($v^+ = 0$, $N^+ = 0$) state of the HD^+ ion in excitation from the intermediate EF $^1\Sigma_u^+$ ($v' = 0$, $N' = 0$) state[3,4] ($v(v^+)$ is the vibrational quantum number and $N(N^+)$ stands for the total angular momentum, excluding spins, of the molecule (ion)). This procedure yielded a value of 124 568.481(12) cm^{-1} in agreement with the theoretical prediction of Kołos (124 568.490 cm^{-1}).[5] In the present experimental study an independent value for the IE of HD is determined from an extrapolation of the *n*p Rydberg series converging to the lowest rotational levels of the first vibrationally excited state ($v^+ = 1$) of the ground electronic state of HD^+. Transitions to these states were measured following a single-photon excitation from the X $^1\Sigma_g^+$ ($v'' = 0$, $J'' = 0$) neutral ground state using the output of a narrow-band tunable vacuum ultraviolet (VUV) laser near 126 500 cm^{-1} (79 nm). The interaction between the $v^+ = 1$, $N^+ = 0$ and 2 Rydberg states with principal quantum number between 15 and 150 is interpreted by MQDT to derive, by extrapolation, the $v^+ = 1$, $N^+ = 0$ and 2 ionization thresholds and, after subtraction of the $v^+ = 1$ vibrational energy of HD^+,[6] the first adiabatic ionization energy of HD. MQDT also permitted the assignment of several low *n*, high v^+ resonances in terms of a Rydberg electron orbital angular momentum *l*-uncoupling frame transformation.[7,8]

The Rydberg states of HD have been much less studied than those of H_2. Takezawa and Tanaka reported the absorption spectrum of HD in the VUV,[9] which is dominated by extensive and strongly perturbed series. Dehmer and Chupka recorded the VUV photoabsorption and photoionization spectra of HD and made many spectral assignments of the Rydberg states converging to the vibrationally excited states of HD^+.[10] The odd *l* Rydberg states of HD have been studied following (2 + 1′) resonance-enhanced three-photon excitation *via* the EF state[3] and spectra of the even *l* Rydberg states have been recorded by (1 + 1′) two-photon excitation *via* the B state.[11]

The high-resolution photoionization spectrum of HD in a supersonic expansion in the range 126 100–126 700 cm^{-1} reported here complements the earlier, classic study of Dehmer and Chupka,[10] who used a noble gas discharge radiation source to monitor the photoionization and photoabsorption of HD in a static gas cell cooled to ~78 K. The simultaneous measurement of these two signal channels allowed an analysis of the highest vibrational levels of the 3pπ D $^1\Pi_u$ state, which are strongly predissociative and could not be observed in the present study. The results of Dehmer and Chupka encouraged Du and Greene to perform an MQDT analysis of the energetic region near the $v^+ = 1$ ionization threshold of HD.[12] Using the rovibrational frame transformation, reformulated in terms of a quantum defect matrix, a good reproduction of the observations of Dehmer and Chupka was obtained, despite the neglect of the energy dependence of the quantum defects, of dissociative channels and of g–u symmetry breaking. Predictions were made of an interesting complex resonance (see ref. 13 for a description of complex resonances) resulting from the interaction between the ($v^+ = 2$) 8pσ(1) interloper state and the ($v^+ = 1$) *n*p2(1) Rydberg series. In the present high-resolution study this feature could be fully resolved and compared with the MQDT prediction.

† Dedicated to Prof. W. A. Chupka on the occasion of his 80th birthday.

 DOI: 10.1039/b302876n

To designate the p Rydberg states at high n values we use the notation $(v^+)\ npN^+(N')$, as above. For the low n states that can be classified in Hund's coupling case (b) we employ the notation $(v^+)\ np\lambda(N')$, where λ (σ or π for a p Rydberg orbital) represents the projection of the Rydberg electron orbital angular momentum along the internuclear axis.

2 Experiment

The experiments were carried out using a narrow bandwidth VUV laser system coupled to a time-of-flight mass spectrometer described in detail in refs. 14 and 15. Near-Fourier-transform-limited VUV laser pulses of wavenumber $\tilde{\nu}_{\mathrm{VUV}}$ are generated at a 25 Hz repetition rate by resonance-enhanced sum-frequency mixing ($\tilde{\nu}_{\mathrm{VUV}} = 2\tilde{\nu}_{\mathrm{A}} + \tilde{\nu}_{\mathrm{B}}$) of two single-mode nanosecond pulsed UV lasers of wavenumbers $\tilde{\nu}_{\mathrm{A}}$ and $\tilde{\nu}_{\mathrm{B}}$ in a krypton gas jet. The resonance enhancement of the sum-frequency mixing is achieved by fixing the tripled output ($\tilde{\nu}_{\mathrm{A}} = 3\tilde{\nu}_1$) of a first dye laser to the $(4p)^6\ {}^1S_0 \rightarrow (4p)^5\ 5p'[1/2]$ ($J = 0$) two-photon resonance of Kr at $2\tilde{\nu}_{\mathrm{A}} = 98\,855.1$ cm^{-1}. Tunable VUV radiation in the range 126 000–127 000 cm^{-1} is obtained by scanning the doubled wavenumber $\tilde{\nu}_{\mathrm{B}} = 2\tilde{\nu}_2$ of a second dye laser in the range 27 640–28 140 cm^{-1}. The two input wavenumbers ($\tilde{\nu}_{\mathrm{A}}$ and $\tilde{\nu}_{\mathrm{B}}$) to the sum-frequency mixing process are produced by tripling and doubling, respectively, the pulsed amplified output of two single-mode ring dye lasers of wavenumber $\tilde{\nu}_1$ and $\tilde{\nu}_2$ in β barium borate (BBO) crystals.

Each pulsed amplification chain consists of three successive dye cells pumped transversally by an injection-seeded Nd:YAG laser. The laser beams exiting the pulsed dye amplifiers are first frequency doubled (or tripled) using one (or two) BBO crystals and then combined at a dichroic mirror before entering the vacuum chamber through a lens ($f = 15$ cm). The beams are focused underneath the orifice of a pulsed nozzle delivering the Kr gas jet. The sum-frequency beam generated by the interaction with the nonlinear gas is separated from the fundamental beams in a vacuum monochromator equipped with a platinum-coated toroidal grating which also refocuses the divergent VUV radiation at the exit hole of the monochromator. 15 cm after the monochromator exit hole, the VUV beam intersects a skimmed supersonic beam of a 10 : 1 Ar : HD (97% isotopically enriched HD, Cambridge Isotope Laboratories, Inc.) gas mixture at a right angle in the middle of an array of resistively coupled cylindrical electrodes with axis parallel to the gas propagation direction. A pulsed electric field of 200 V cm^{-1} is applied 1 μs after each VUV laser shot to extract the HD^+ ions produced by single-photon ionization through a time-of-flight tube toward a micro channel plate detector. The photoionization spectrum of HD was recorded by monitoring the HD^+ ion signal as a function of the VUV laser wavenumber.

The VUV wavenumber is determined from the cw output wavenumbers, $\tilde{\nu}_1$ and $\tilde{\nu}_2$, of the ring dye lasers by building the sum $6\tilde{\nu}_1 + 2\tilde{\nu}_2$ ($= 2\tilde{\nu}_{\mathrm{A}} + \tilde{\nu}_{\mathrm{B}}$). To avoid drifts in the wavenumber of the first ring dye laser, its frequency is locked to the position $\tilde{\nu}_1 = 16\,475.8492(15)$ cm^{-1} as described in ref. 15. The wavenumber $\tilde{\nu}_2$ of the second ring dye laser is calibrated to an accuracy of better than 0.002 cm^{-1} by recording (a) laser induced fluorescence spectra of molecular iodine, and (b) the transmission through two étalons of different free spectral ranges. An uncertainty of 0.009 cm^{-1} in the VUV wavenumber results from the stabilization and calibration procedure.

The chirp shifts that may arise in pulsed amplification chains[16,17] and nonlinear frequency up-conversion processes were neither directly measured nor compensated but were estimated to be at most 0.01 cm^{-1} in the VUV from the observed variation of the VUV wavenumber when modifying the dye concentrations and mixing ratios in the amplification chains and varying the Nd:YAG power and the density of the nonlinear gas.

The stray electric fields in the photoexcitation region were measured by millimeter wave spectroscopy following the method described in ref. 18 and were kept below 3 mV cm^{-1} so that Stark shifts of the transition frequencies to Rydberg states with $n < 150$ are negligible. Possible Doppler shifts caused by a deviation from 90° of the angle between VUV laser beam and probe gas beams were reduced to less than 0.002 cm^{-1} by a careful alignment of both beams. Finally, the pressure shifts in the positions of the high Rydberg states were found to be completely negligible under our experimental conditions. Our error budget is thus dominated by the uncertainty in the chirp shifts and by the uncertainty in the calibration procedure and leads to an overall (conservative) uncertainty of 0.014 cm^{-1}.

The rotational temperature of the HD gas in the skimmed supersonic expansion was estimated to be ~25 K by comparing the relative intensities of transitions originating from the $J'' = 0$ and 1 rotational levels of the $X\ {}^1\Sigma_g^+$ ($v'' = 0$) ground state of HD with the relative intensities in the 78 K spectrum reported by Dehmer and Chupka.[10] At 25 K, the intensities of transitions out of $J'' \geq 2$ ground state levels are negligible.

3 Results and discussion

3.1 Overall description of the spectrum

The photoionization spectrum of HD in the vicinity of the $X\ {}^2\Sigma_g^+$ ($v^+ = 1$) ionization threshold is displayed in Fig. 1. The spectrum was recorded by monitoring the HD^+ ions produced either by direct ionization or autoionization in the $v^+ = 0$ continuum (and above 126 481 cm^{-1} also in the $v^+ = 1$ continuum) following single-photon excitation from the ground neutral state. The spectrum reveals a large number of resonances with varying widths and shapes and is similar, in its irregularities, to the corresponding spectrum of H_2.[8,19] The positions and widths of the resonances are listed with their assignments in Tables 1–3. The narrowest lines in the spectrum, with widths of about 0.025 cm^{-1}, are significantly broader than the VUV laser bandwidth. The broadening may be caused by either a residual Doppler broadening or by the lifetime of the Rydberg states.

The low wavenumber side of the spectrum is dominated by transitions to high members (with $n > 15$) of the interacting ($v^+ = 1$) $np0(1)$ and $np2(1)$ Rydberg series (see Tables 1 and 2, respectively). No transitions from $J'' = 0$ to ($v^+ = 1$) $np1$ or $np3$ Rydberg states are observed, giving no evidence of significant g–u symmetry breaking. The rotational channel interaction between these series leads to the window resonances characteristic of the photoionization of molecular hydrogen.[8,20] In the absence of additional interactions, these window resonances are a consequence of the fact that the transitions to the $np0(1)$ Rydberg states are strong and those to the $np2(1)$ Rydberg states have very weak intensities. The rotational channel interaction results in intensity minima around the positions of the $np2(1)$ resonances that are usually observed in the continuum above the $N^+ = 0$ threshold but also modify the intensity distribution below this threshold, as clearly observed in Fig. 1 between 126 400 and 126 470 cm^{-1}. Analysis of these structures by MQDT leads to the determination of the $v^+ = 1$, $N^+ = 0$ and 2 ionization thresholds as will be shown below.

The direct ionization into the $v^+ = 1$ continuum is hardly visible on the intensity scale of Fig. 1. One would therefore not expect to see the $np2(1)$ series above the $N^+ = 0$ series limit, because the series would appear as a regular sequence of window resonances in this very weak continuum. However,

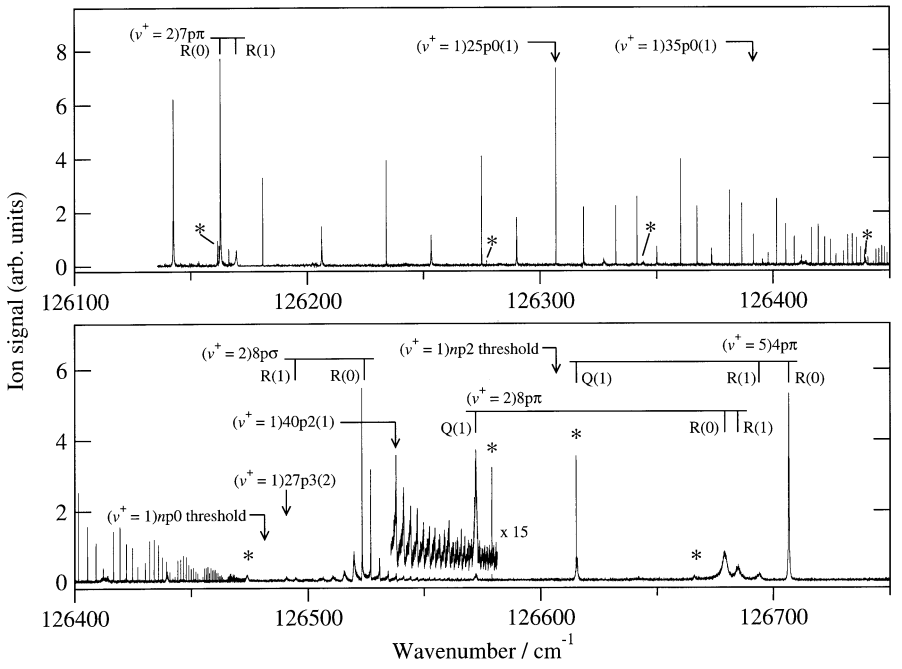

Fig. 1 Photoionization spectrum of the *n*p Rydberg series in the region of the HD^+ X $^2\Sigma_g^+$ ($v^+ = 1$) threshold. At the low temperature of the supersonic expansion ($T_{rot} \approx 25$ K), only transitions from the $J'' = 0$ and 1 rotational levels of the ground vibronic state of HD are observed. Lines marked with an asterisk represent unassigned transitions.

a strong interaction of the *n*p2(1) series with the ($v^+ = 2$) 8pσ(1) interloper state lends considerable intensity to the *n*p2(1) resonances between 126 500 and 126 575 cm^{-1} and causes their profiles to strongly deviate from those typical of window resonances. The resulting complex resonance has already been observed at lower resolution by Dehmer and Chupka[10] and analyzed by Du and Greene using MQDT.[12] At high resolution and on an expanded scale (see Fig. 2[21]), several interesting features of this complex resonance become observable, in particular the narrowing of the *n*p2(1) lines that takes place in the immediate vicinity of the interloper at ~126 525 cm^{-1} and the abrupt change in the degradation of the Fano profiles as one passes through the center of the complex resonance.

The experimental spectrum is in excellent agreement with an as yet untested prediction of the complex resonance made by Du and Greene[12] using MQDT, which is reproduced in the lower half of Fig. 2.[21] The theoretical spectrum was obtained after convolution over an assumed experimental resolution of 0.01 cm^{-1}. Not only the reversal of the Fano profiles, but also the line widths and relative intensities, are accurately predicted by the calculation. This comparison documents the predictive power of MQDT.

The observation of the *n*p2(1) series beyond the $N^+ = 0$ ionization threshold provides further information that can be used to derive the $N^+ = 2$ series limit (see below). The positions and widths of the ($v^+ = 1$) *n*p2(1) resonances listed in Table 2 were derived by fitting a series of Fano lineshapes to the experimental data.

In addition to the dominant spectral features mentioned above, several isolated lines are observed in Fig. 1 that can be attributed to low *n* Rydberg states converging on vibrationally excited levels of the X $^2\Sigma_g^+$ ground state of HD^+ or to transitions from the $J'' = 1$ ground state level. These lines are listed in Table 3 with their assignments, several of which were adopted from the previous work of Dehmer and Chupka[10] and Du and Greene.[12] The remaining assignments in Table 3 were made on the basis of model MQDT calculations described below. Most of these isolated resonances correspond to transitions to $v^+ = 2$ Rydberg states although transitions to $v^+ = 5$ Rydberg states also appear in the region investigated here. Several transitions, with positions listed in Table 3, remain unassigned and are indicated by asterisks in Fig. 1.

3.2 Determination of the ionization energy of HD and MQDT calculations

The assignment of several low *n* resonances and the determination of the ionization energy of HD were reached on the basis of simple multichannel quantum defect theory (MQDT) calculations.

Our MQDT analysis of the ($v^+ = 1$) *n*p0(1) and *n*p2(1) series was primarily aimed at interpreting the intensity distribution below the $v^+ = 1$, $N^+ = 0$ threshold and determining the exact positions of the $v^+ = 1$, $N^+ = 0$ and 2 ionization thresholds. The analysis is based on eqn. (1)

$$\sum_{N_j^+} \left[\tan(\pi \nu_{N_i^+}) \delta_{N_i^+ N_j^+} + K_{N_i^+ N_j^+} \right] Z_{N_j^+} = 0 \qquad (1)$$

which has been used in previous MQDT studies, for instance of the Rydberg spectrum of N_2.[22] This equation describes the interaction between the *n*p channels characterized by the core rotational quantum number N_i^+ and N_j^+. In eqn. (1), $\nu_{N_i^+}$ represents the effective principal quantum number with respect to the N_i^+ ionization channel, and $Z_{N_j^+}$ corresponds to the channel mixing coefficient of the N_j^+ channel.

The non-diagonal reactance matrix $K_{N_i^+ Nj^+}$ takes the short-range interactions into account in the form of Hund's case (b) $\mu_{p\sigma}$ and $\mu_{p\pi}$ quantum defects which can be converted into Hund's case (d) quantum defects by the *l*-uncoupling transformation $\langle N^+|\lambda\rangle^{(l,N)}$ the expression of which is given, for instance, in equation (4) of ref. 23.

Our calculation of the positions of the ($v^+ = 1$) *n*pN^+(1) resonances did not include interactions with channels associated with other vibrational channels of the HD^+ ion. Interaction with the $v^+ = 0$ channels, which gives rise to vibrational autoionization of the $v^+ = 1$ Rydberg states, indeed only affects their widths but not their positions. The effects of the interactions with the $v^+ > 1$ channels (mostly

Table 1 Positions, widths (FWHM) and relative intensities of the transitions from the ground X $^1\Sigma_g^+(v'' = 0, J'' = 0)$ state of HD to the *n*p Rydberg states belonging to the $(v^+ = 1)$ *n*p0(1) series. The experimental results are compared with the results of MQDT calculations, from which the $N^+ = 0$ channel mixing coefficient, Z_0, and intensities were determined. The attribution of the Rydberg states to the $(v^+ = 1)$ *n*p0(1) series rather than the $(v^+ = 1)$ *n*p2(1) series was made on the basis of the magnitude of the channel mixing coefficient. The intensities of the experimental lines are given as the product of their widths and heights

	Transition wavenumber/cm^{-1}				
n	Exp	Exp. − Calc.[a]	Width/ cm^{-1}	Relative intensities	$\|Z_0\|^2$
18[b]	126142.490	−0.158	0.168	28.111	0.964
19[b]	126180.983	0.082	0.039	4.790	0.594
20[b]	126206.180	0.465	0.213	7.196	0.994
21	126234.040	0.022	0.051	5.108	0.776
22[b]	126253.365	0.324	0.234	6.789	0.939
23	126274.937	0.010	0.049	5.122	0.809
24[b]	126289.944	0.216	0.185	7.059	0.951
25	126306.880	0.000	0.036	6.768	0.734
26[b]	126318.732	0.103	0.091	4.593	1.000
27	126332.559	0.000	0.043	2.615	0.467
28	126341.609	0.031	0.051	3.365	0.943
29	126350.057	0.120	0.153	2.250	0.817
30	126360.233	−0.004	0.031	3.080	0.682
31	126367.254	0.024	0.055	3.170	0.975
32	126373.517	0.074	0.122	1.940	0.763
33	126381.337	−0.006	0.030	2.063	0.613
34	126386.629	0.009	0.040	2.401	0.933
35	126391.602	0.033	0.064	1.882	0.975
36	126398.001	−0.010	0.061	0.582	0.196
37	126401.633	−0.003	0.030	1.896	0.732
38	126405.519	0.007	0.040	1.606	0.948
39	126409.143	0.017	0.050	1.371	0.987
40	126412.230	0.031	0.170	1.351	0.449
41	126416.612	0.012	0.030	1.097	0.514
42	126419.412	−0.003	0.032	1.297	0.825
43	126422.134	0.000	0.037	1.000	0.963
44	126424.677	0.005	0.044	0.979	0.993
45	126426.960	0.012	0.065	0.594	0.701
46	126430.180	−0.018	0.038	0.483	0.200
47	126432.028	−0.007	0.031	0.862	0.603
48	126433.950	−0.003	0.029	0.853	0.822
49	126435.803	0.002	0.033	0.721	0.937
50	126437.549	−0.002	0.035	0.598	0.995
51	126439.190	0.005	0.050	0.576	0.970
52	126440.680	0.001	0.047	0.299	0.699
53	126441.950	0.006	0.047	0.056	0.126
54	126444.098	−0.012	0.033	0.459	0.359
55	126445.331	−0.011	0.033	0.498	0.628
56	126446.562	−0.004	0.027	0.451	0.789
57	126447.748	0.003	0.029	0.461	0.889
58	126448.876	0.006	0.036	0.386	0.954
59	126449.937	−0.005	0.028	0.256	0.992
60	126450.966	0.008	0.034	0.297	0.996
61	126451.918	0.001	0.042	0.284	0.935
62	126452.812	−0.002	0.035	0.139	0.729
63	126453.624	−0.007	0.052	0.062	0.329
64	126454.976	−0.024	0.049	0.156	0.059
65	126455.678	−0.011	0.030	0.215	0.274
66	126456.396	−0.007	0.035	0.348	0.485
67	126457.113	0.000	0.030	0.322	0.639
68	126457.801	−0.003	0.032	0.242	0.747
69	126458.466	−0.004	0.027	0.258	0.824
70	126459.113	0.002	0.034	0.284	0.882
71	126459.724	−0.004	0.033	0.275	0.926
72	126460.318	−0.002	0.028	0.223	0.959
73	126460.886	−0.002	0.035	0.223	0.983
74	126461.425	−0.008	0.030	0.131	0.997
75	126461.950	−0.007	0.031	0.099	0.999
76	126462.455	−0.003	0.033	0.105	0.981
77	126462.936	−0.004	0.031	0.111	0.934
78	126463.394	−0.006	0.031	0.086	0.842
79	126463.834	−0.005	0.041	0.049	0.686
80		126464.256			0.462
81		126464.648			0.218
82		126465.014			0.047
83	126465.681	−0.017	0.030	0.072	0.059
84	126466.025	−0.011	0.029	0.092	0.172
85	126466.364	−0.010	0.027	0.097	0.297
86	126466.702	−0.005	0.028	0.122	0.411
87	126467.028	−0.006	0.031	0.123	0.508
88	126467.351	−0.002	0.030	0.107	0.588
89	126467.663	0.000	0.031	0.074	0.653
90	126467.964	0.000	0.024	0.086	0.708
91	126468.255	0.000	0.025	0.070	0.753
92	126468.544	0.005	0.024	0.086	0.792
93	126468.812	0.000	0.030	0.060	0.824
94	126469.082	0.003	0.034	0.068	0.853
95	126469.343	0.006	0.025	0.060	0.877
96	126469.589	0.003	0.025	0.060	0.899
97	126469.829	0.000	0.031	0.062	0.918
98	126470.071	0.006	0.028	0.056	0.934
99	126470.296	0.003	0.027	0.054	0.949
100	126470.519	0.005	0.028	0.056	0.962
101	126470.730	0.001	0.029	0.046	0.973
102	126470.939	0.001	0.030	0.048	0.982
103	126471.140	−0.001	0.030	0.036	0.989
104	126471.337	−0.001	0.033	0.039	0.995
105	126471.530	0.002	0.034	0.041	0.998
106	126471.717	0.002	0.030	0.036	1.000
107	126471.896	0.000	0.031	0.037	0.999
108	126472.073	0.001	0.028	0.045	0.996
109	126472.241	−0.001	0.036	0.057	0.989
110	126472.411	0.003	0.029	0.058	0.980
111	126472.579	0.009	0.028	0.056	0.966
112	126472.730	0.003	0.028	0.045	0.948
113	126472.879	−0.002	0.027	0.043	0.924
114	126473.031	0.002	0.027	0.043	0.895
115	126473.177	0.002	0.027	0.043	0.859
116		126473.316			0.816
117		126473.453			0.766
118		126473.587			0.707
119		126473.718			0.640
120		126473.845			0.566
121		126473.968			0.486
122		126474.089			0.405
123		126474.206			0.323
124		126474.320			0.244
125		126474.430			0.171
126		126474.539			0.110
127		126474.644			0.062
128		126474.747			0.028
129		126474.847			0.008
130		126475.041			0.004
131	126475.128	−0.006	0.021	0.017	0.017
132		126475.227			0.038
133		126475.317			0.064
134	126475.403	−0.002	0.026	0.021	0.094
135	126475.491	−0.002	0.055	0.022	0.127
136	126475.577	−0.002	0.035	0.028	0.160
137	126475.662	−0.001	0.038	0.030	0.194
138	126475.747	0.002	0.042	0.033	0.229
139	126475.834	0.008	0.041	0.016	0.262
140	126475.904	−0.001	0.039	0.016	0.294
141	126475.987	0.004	0.041	0.016	0.326
142	126476.065	0.006	0.036	0.014	0.354
143	126476.138	0.004	0.053	0.021	0.383
144		126476.207			0.409
145	126476.276	−0.003	0.046	0.018	0.435
146	126476.356	0.006	0.046	0.018	0.458

[a] When the experimental value is missing the calculated position is given instead of the difference. [b] Obviously perturbed experimental positions. A zero weight was given to these positions when fitting the MQDT parameters.

Table 2 Positions, widths (FWHM) and relative intensities of the transitions from the ground X $^1\Sigma_g^+(v''=0,\ J''=0)$ state of HD to the *n*p Rydberg states belonging to the $(v^+=1)$ *n*p2(1) series. The experimental results are compared with the results of MQDT calculations, from which the $N^+=2$ channel mixing coefficient, Z_2, and intensities were determined. The attribution of the Rydberg states to the $(v^+=1)$ *n*p2(1) series rather than the $(v^+=1)$ *n*p0(1) series was made on the basis of the magnitude of the channel mixing coefficient. The intensities of the experimental lines are given as the product of their widths and heights

	Transition wavenumber/cm^{-1}				
n	Exp.	Exp. − Calc.[a]	Width/ cm^{-1}	Relative intensities	$\lvert Z_2\rvert^2$
16[b]	126166.397	−0.627	0.078	1.302	0.868
17		126220.233			1.000
18		126263.121			0.978
19		126298.168			0.996
20	126327.366	0.320	0.416	3.141	0.907
21		126354.776			0.983
22		126377.227			0.989
23	126395.522	0.070	0.139	0.552	0.804
24		126414.271			0.971
25		126428.715			0.966
26	126442.960	−0.019	0.079	0.220	0.955
27		126454.344			0.978
28		126465.360			0.999
29		126481.388			1.000
30		126483.646			—
31		126491.504			—
32		126498.633			—
33		126505.121			—
34[b]	126510.660	−0.382	1.843	5.341	—
35[b]	126515.426	−1.035	1.184	9.471	—
36[b]	126519.610	−1.823	0.787	14.010	—
[c]	126523.200	—	0.095	14.178	—
37[b]	126526.938	0.933	0.100	7.875	—
38[b]	126530.774	0.554	0.245	3.994	—
39[b]	126534.505	0.392	0.347	2.258	—
40[b]	126538.006	0.289	0.348	1.678	—
41[b]	126541.280	0.220	0.367	1.220	—
42[b]	126544.338	0.173	0.384	1.021	—
43[b]	126547.206	0.150	0.322	0.688	—
44[b]	126549.869	0.117	0.307	0.525	—
45[b]	126552.393	0.124	0.321	0.543	—
46[b]	126554.731	0.108	0.229	0.352	—
47[b]	126556.937	0.109	0.298	0.379	—
48[b]	126558.985	0.089	0.204	0.263	—
49[b]	126560.811	−0.027	0.375	0.466	—
50[b]	126562.713	0.048	0.164	0.168	—
51[b]	126564.442	0.057	0.185	0.164	—
52	126566.035	0.028	0.138	0.173	—
53	126567.552	0.015	0.148	0.125	—
54	126569.018	0.035	0.099	0.088	—
55		126570.350			—
56		126571.645			—
57		126572.871			—
58		126574.035			—
59	126575.188	0.048	0.139	0.065	—
60	126576.261	0.071	0.152	0.063	—
61	126577.213	0.024	0.122	0.082	—
62	126578.162	0.022	0.103	0.059	—
63		126579.045			—
64		126579.909			—
65		126580.733			—
66		126581.519			—
67	126582.230	−0.040	0.084	0.051	—
68	126582.964	−0.025	0.125	0.059	—
69	126583.646	−0.030	0.077	0.055	—
70	126584.380	0.045	0.081	0.029	—
71	126584.981	0.015	0.107	0.039	—
72	126585.585	0.015	0.064	0.020	—
73	126586.166	0.017	0.089	0.017	—
74	126586.700	−0.005	0.104	0.017	—
75	126587.230	−0.010	0.089	0.020	—
76	126587.752	−0.001	0.127	0.017	—
77	126588.226	−0.020	0.104	0.042	—
78	126588.701	−0.019	0.126	0.025	—
79	126589.152	−0.024	0.123	0.024	—
80	126589.597	−0.019	0.053	0.013	—
81	126590.011	−0.028	0.248	0.029	—
82	126590.406	−0.041	0.137	0.006	—
83	126590.845	0.005	0.119	0.010	—
84	126591.243	0.025	0.060	0.003	—

[a] When the experimental value is missing the calculated position is given instead of the difference. [b] Obviously perturbed experimental positions. A zero weight was given to these positions when fitting the MQDT parameters. [c] The line at 126 523.200 cm^{-1} is the most intense member of the complex resonance and is taken to represent the position of the $(v^+=2)$ 8pσ(1) interloper state, see Table 3.

$v^+=2$ and 5 in the region of the $v^+=1$ ionization threshold) cannot be neglected, but can be treated qualitatively using eqn. (1) by including suitable channels with adjustable parameters describing the vibrational channel interactions. Although the inclusion of such channels is helpful in identifying and modeling local perturbations in the $(v^+=1)$ *n*p0(1) and *n*p2(1) series, it did not have a significant effect on the extrapolation of the series limits nor on the determination of the case (b) quantum defects of the $(v^+=1)$ *n*p channels, first because the positions of the thresholds are predominantly defined by the high *n* Rydberg levels (with *n* up to 146 for the $(v^+=1)$ *n*p0(1) and up to 84 for the $(v^+=1)$ *n*p2(1) channels), and second because the obviously perturbed levels were given a zero weight in the final fits (see Tables 1 and 2). The MQDT analysis also considered the positions of several of the $(v^+=1)$ *n*p2(1) resonances above the $N^+=0$ threshold listed in Table 2.

The relative intensities below the $v^+=1$, $N^+=0$ series limit were calculated from the channel mixing coefficients using eqn. (2)

$$I=\left(\sum_{N_i^+}\frac{Z_{N_i^+}+D_{N_i^+}}{\nu_{N_i^+}^{3/2}}\right)^2 \qquad (2)$$

where $D_{N_i}{}^+$ represents the dipole transition amplitude (from the X $^1\Sigma_g^+$ $(v''=0,\ J''=0)$ state) to the $N_i{}^+$ channel, which can be calculated by applying the *l*-uncoupling transformation to the case (b) dipole moments, as described in ref. 23. The case (b) dipole moments, $D^{\sigma(N=1)}_{\Sigma(J=0)}$ and $D^{\pi(N=1)}_{\Sigma(J=0)}$, were calculated assuming the radial dipole integrals $a^{p\sigma}_{s\Sigma}$ and $a^{p\pi}_{s\Sigma}$ are of equal magnitude.[23] The calculated and measured spectra of the two interacting $(v^+=1)$ *n*p$(N^+=0,\ 2)$ series below the $v^+=1$, $N^+=0$ threshold are compared in Fig. 3. Overall, the calculated intensity distribution agrees well with the experimental spectrum. However, the window resonances appear degraded in the opposite direction in calculated (inverted stick spectrum) and experimental (upper trace) spectra. The most likely explanation for this discrepancy is the effect of the broad $(v^+=2)$ 8pσ(1) complex resonance located just above the $v^+=1$, $N^+=0$ threshold (see above). Indeed, MQDT calculations which include all open and closed vibrational channels appear to correctly describe the intensity distribution.[21]

Table 4 lists the set of MQDT parameters that resulted for the $(v^+=1)$ *n*pN^+(1) channels from a fit of the model

Table 3 Positions, widths and assignments of transitions to low n interloper states belonging to Rydberg series converging to $v^+ = 1$, $N^+ = 3$ and $v^+ = 2$ and 5 ionization thresholds of HD. Where possible MQDT calculated transition energies are also given. The table also lists the positions of several unassigned transitions observed between 125100–125700 cm^{-1}. All values are given in cm^{-1}

Assignment	Exp.	Calc.[a]	Width	Reference
$v^+ = 1$				
27p3, R(1)[b]	126490.733	126489.929	0.908	12
$v^+ = 2$				
7pπ, R(0)	126162.814	126161.696	0.193	
7pπ, R(1)	126169.650	126165.114	0.512	
8pσ, R(0)[c]	126523.200	126524.990	~18	~126530,[12]
8pσ, R(1)	126494.710	126494.428	0.714	12
8pπ, R(0)	126679.040	126673.022	2.601	
8pπ, R(1)	126684.689	126681.087	1.902	
8pπ, Q(1)	126572.131	126571.352	0.853	126574,[10]
$v^+ = 5$				
4pπ, R(0)	126706.593		0.349	126704,[10]
4pπ, R(1)	126694.010		1.901	126693,[10]
4pπ, Q(1)	126615.525		0.797	126614,[10]
Unassigned				
	126161.487		0.044	
	126162.154		0.040	
	126277.045		0.053	
	126344.277		0.874	
	126439.541		0.607	
	126473.969		0.800	
	126578.968		0.048	
	126615.260		0.085[d]	
	126665.956		0.757	

[a] Energetic positions of the ($v^+ = 1$) 27p3(2) and ($v^+ = 2$) np Rydberg states were calculated using the $v^+ = 1$ quantum defects and threshold determined in this work and the rotational spacing in the HD^+ ($v^+ = 1$) state from ref. 6. The ($v^+ = 2$) np series quantum defects were estimated from a linear extrapolation of the ($v^+ = 0$) np ($\mu_{p\sigma} = 0.2012$ and $\mu_{p\pi} = -0.0832$,[3] and ($v^+ = 1$) np (see Table 4) series quantum defects. [b] No other members of the ($v^+ = 1$) np1 or np3 series are observed in the spectra, presumably due to the minor population of the $J'' = 1$ level of the ground vibronic state of HD. The transition to the ($v^+ = 1$) 27p3(2) state observed here appears to gain intensity by coupling to the nearby ($v^+ = 2$) 8pσ(2) state. [c] The central position of the ($v^+ = 2$) 8pσ R(0) resonance is difficult to locate because of the unusual profile of the complex resonance resulting from the interaction of the ($v^+ = 2$) 8pσ(1) state with the ($v^+ = 1$) np2(1) series, and so is taken here as the position of the most intense line in the complex resonance. It should also be noted that the width given here is the estimated overall width of the complex resonance, while the individual lines within the resonance are much narrower, see Table 2. [d] The broad feature underlying this line has been assigned as the ($v^+ = 5$) 4pπ Q(1) transition.

described above to the experimental positions. The line positions calculated from these parameters are compared with the experimental ones in Tables 1 and 2. Overall the deviations between measured and calculated positions are comparable to, or less than the widths of the resonances. Clearly perturbed transitions close to the positions of the interloper states are obviously not well predicted by the calculations.

The case (b) quantum defects for the ($v^+ = 1$) np channels of HD ($\mu_{p\sigma} = 0.2390(51)$ and $\mu_{p\pi} = -0.0854(12)$) determined in the MQDT fit lie close to both the values determined by Gilligan and Eyler[3] for the ($v^+ = 0$) np channels of HD ($\mu_{p\sigma} = 0.2012$, $\mu_{p\pi} = -0.0832$) and to the values derived for the ($v^+ = 1$) np channels of H_2 ($\mu_{p\sigma} = 0.230$ and $\mu_{p\pi} = -0.085$).[8] This good agreement provides a justification for the strongly simplified MQDT model described above. Additional supporting evidence for the validity of these parameters was provided by a linear extrapolation of the quantum defects of the $v^+ = 0$ and 1 channels of HD to the $v^+ = 2$ channel on the basis of which the positions of the ($v^+ = 2$) 7pπ, 8pσ and 8pπ interlopers could be satisfactorily predicted, as is illustrated by the results presented in Table 3.

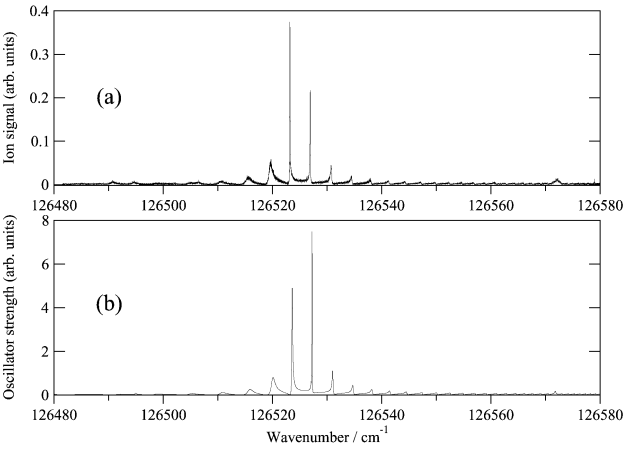

Fig. 2 Comparison of the high resolution VUV photoionization spectrum of HD in the region of the ($v^+ = 2$) 8pσ(1) complex resonance (a) with the MQDT prediction of Hamilton, Du and Greene[12,21] (b).

The $v^+ = 1$, $N^+ = 0$ and 2 ionization thresholds could be determined in the fit procedure with an uncertainty (3σ) of 0.011 and 0.09 cm^{-1}, respectively. Considering the sources of systematic errors described in Section 2, the absolute position of the $v^+ = 1$, $N^+ = 0$ threshold relative to the $v'' = 0$, $J'' = 0$ ground vibrational level of HD can be determined to be $126\,481.486 \pm 0.017$ cm^{-1}.

When combined with the energy difference of 1912.9953 cm^{-1} between the $v^+ = 1$, $N^+ = 0$ and the $v^+ = 0$, $N^+ = 0$ levels of HD^+ determined by Moss,[6] in what is up to now the most sophisticated theoretical treatment of the rovibrational energy level structure of HD^+, the position of the $v^+ = 1$, $N^+ = 0$ threshold enables the derivation of a new value of the adiabatic ionization energy of HD

$$\mathrm{IE} = 124\,568.491 \pm 0.017\ \mathrm{cm}^{-1}, \quad (3)$$

the uncertainty of which is limited by that of the chirp shift arising in the pulsed amplification chains and non-linear frequency up-conversion processes (see Section 2). It should be

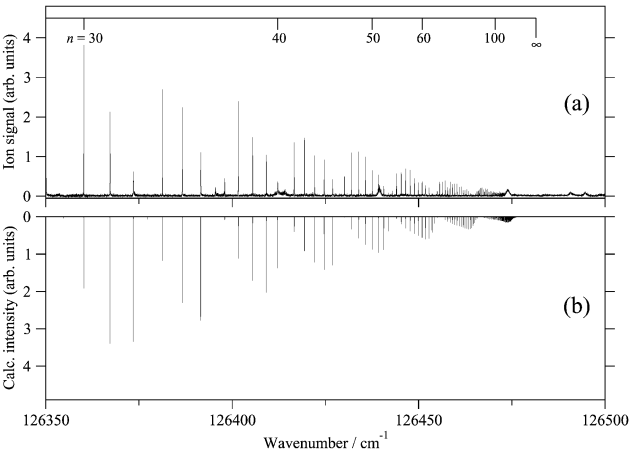

Fig. 3 Photoionization spectrum (a) and MQDT simulation (b) of the np Rydberg series converging to the $v^+ = 1$, $N^+ = 0$ level of the ground electronic state of the HD^+ ion. Note that the calculated spectrum does not include the effect of the varying width in the experimental spectrum.

Table 4 MQDT parameters obtained from a fit to the observed line positions of the *n*p Rydberg series converging to the $v^+ = 1$, $N^+ = 0$ and 2 limits of the ground electronic state of HD^+. The series limits are given relative to the ground rovibronic state of HD. The quantum defect energy dependence was ignored in these calculations because only levels with of $n > 15$ were included. The uncertainties in the fitted parameters are given as one standard deviation

$N^+ = 0$ limit	126481.4862(36) cm^{-1}
$N^+ = 2$ limit	126606.822(20) cm^{-1}
$\mu_{p\sigma}$	0.2388(53)
$\mu_{p\pi}$	−0.0855(12)
RMS of fit = 0.2520	

noted that Moss' calculations[6] agree with the infrared measurement of Wing *et al.*[24] to within 0.001 cm^{-1}. The infrared spectrum of HD^+ revealed in addition that the spin–rotation and hyperfine interactions induce splittings of the order of 0.0015 cm^{-1}.[24]

4 Conclusions

The single-photon photoionization spectrum of HD has been recorded at high resolution using a near-Fourier-transform-limited VUV laser system and the positions, widths and shapes of a large number of autoionizing resonances have been measured in the vicinity of the $v^+ = 1$ threshold of HD^+. The general appearance of the spectrum below the $v^+ = 1$, $N^+ = 0$ threshold is well reproduced by MQDT calculations although the degradation of the *n*p2 window resonances appear to be affected by the very broad ($v^+ = 2$) 8pσ(1) complex resonance centered more than 40 cm^{-1} above the first ionization threshold. The recording of this complex resonance at high resolution was found to be in excellent agreement with an as yet untested MQDT prediction made by Du and Greene.[12] The *n*p Rydberg series converging to the $v^+ = 1$, $N^+ = 0$ and 2 ionization thresholds have been observed up to *n* values of 150. The observation of such high Rydberg states has enabled the derivation, from an MQDT fit, of a new value of the adiabatic ionization energy of HD (IE = 124 568.491 ± 0.017 cm^{-1}). This new value, compared with earlier values in Table 5, is consistent both with the value derived by Eyler and coworkers[3,4] from measurements of the $v^+ = 0$ Rydberg states following $2 + 1'$ three-photon excitation *via* the EF intermediate state and with the latest theoretical prediction of Kołos.[5]

Table 5 Comparison of experimental and theoretical values of the adiabatic ionization energy (IE) of HD

IE/cm^{-1}	Reference
124568.5 ± 0.6[a]	Experiment[9]
124568.481(12)	Experiment[3,4]
124568.491 ± 0.017	This work
124568.490	Theory[5]

[a] After correcting for the pressure shift, as suggested in Ref. 25.

Acknowledgements

We thank E. L. Hamilton and C. H. Greene (University of Colorado, JILA, Boulder) for kindly recalculating the HD photoionization spectrum of ref. 12 for inclusion in Fig. 2 of the present article. This work is supported financially by the Swiss National Science Foundation and the ETH Zürich. W.U. wishes to thank the Laboratorium für Physikalische Chemie at the ETH for the hospitality and support during a sabbatical stay in Zurich.

References

1 A. de Lange, E. Reinhold and W. Ubachs, *Int. Rev. Phys. Chem.*, 2002, **21**, 257.
2 A. Balakrishnan, M. Vallet and B. P. Stoicheff, *J. Mol. Spectrosc.*, 1993, **162**, 168.
3 J. M. Gilligan and E. E. Eyler, *Phys. Rev. A*, 1992, **46**, 3676.
4 D. Shiner, J. M. Gilligan, B. M. Cook and W. Lichten, *Phys. Rev. A*, 1993, **47**, 4042.
5 W. Kołos, *J. Chem. Phys.*, 1994, **101**, 1330.
6 R. E. Moss, *Mol. Phys.*, 1993, **78**, 371.
7 E. S. Chang and U. Fano, *Phys. Rev. A*, 1972, **6**, 173.
8 G. Herzberg and Ch. Jungen, *J. Mol. Spectrosc.*, 1972, **41**, 425.
9 S. Takezawa and Y. Tanaka, *J. Chem. Phys.*, 1972, **56**, 6125.
10 P. M. Dehmer and W. A. Chupka, *J. Chem. Phys.*, 1983, **79**, 1569.
11 F. Merkt, H. Xu and R. N. Zare, *J. Chem. Phys.*, 1996, **104**, 950.
12 N. Y. Du and C. H. Greene, *J. Chem. Phys.*, 1986, **85**, 5430.
13 Ch. Jungen and M. Raoult, *Faraday Discuss.*, 1981, **71**, 253.
14 U. Hollenstein, H. Palm and F. Merkt, *Rev. Sci. Instrum.*, 2000, **71**, 4023.
15 U. Hollenstein, R. Seiler and F. Merkt, *J. Phys. B: At. Mol. Opt. Phys.*, 2003, **36**, 893.
16 E. E. Eyler, A. Yiannopoulou, S. Gangopadhyay and N. Melikechi, *Opt. Lett.*, 1997, **22**, 49.
17 K. S. E. Eikema, W. Ubachs, W. Vassen and W. Hogervorst, *Phys. Rev. A*, 1997, **55**, 1866.
18 A. Osterwalder and F. Merkt, *Phys. Rev. Lett.*, 1999, **82**, 1831.
19 P. M. Dehmer and W. A. Chupka, *J. Chem. Phys.*, 1976, **65**, 2243.
20 U. Fano, *Phys. Rev. A*, 1970, **2**, 353.
21 E. L. Hamilton and C. H. Greene, personal communication, Hamilton and Greene have recalculated the HD photoionization spectrum of ref. 12 in the region of the complex resonance for comparison with our experimental spectrum in Fig. 2.
22 K. P. Huber and Ch. Jungen, *J. Chem. Phys.*, 1990, **92**, 850.
23 K. P. Huber, Ch. Jungen, K. Yoshino, K. Ito and G. Stark, *J. Chem. Phys.*, 1994, **100**, 7957.
24 W. H. Wing, G. A. Ruff, W. E. Lamb and J. J. Spezeski, *Phys. Rev. Lett.*, 1976, **36**, 1488.
25 I. Dabrowski and G. Herzberg, *Can. J. Phys.*, 1976, **54**, 525.